Turkish Journal of Electrical Engineering & Computer Sciences

http://journals.tubitak.gov.tr/elektrik/

Research Article

Turk J Elec Eng & Comp Sci
(2016) 24: 2084 – 2105

doi:10.3906/elk-1312-59

Modeling and rotor field-oriented control of a faulty three-phase induction motor based on GSA for tuning of PI controllers

Mohammad JANNATI[1], Ali MONADI[1,*], Nik Rumzi NIK IDRIS[1], Ahmad Athif MOHD FAUDZI[2], Frede BLAABJERG[3]

[1]UTM-PROTON Future Drive Laboratory, Faculty of Electrical Engineering, Universiti Teknologi Malaysia, Johor Bahru, Malaysia

[2]Centre for Artificial Intelligence and Robotics (CAIRO), Universiti Teknologi Malaysia, Johor Bahru, Malaysia

[3]Department of Energy Technology, Aalborg University, Aalborg East, Denmark

Received: 08.12.2013 • **Accepted/Published Online:** 05.07.2014 • **Final Version:** 15.04.2016

Abstract: This paper discusses the d-q model and winding function method (WFM) for modeling and a rotor field-oriented control (RFOC) system for controlling a faulty three-phase induction motor (three-phase IM when one of the phases is disconnected). In the adapted scheme for controlling the faulty IM, it is necessary for the PI controller coefficients to change. For this purpose, the gravitational search algorithm (GSA) is used for tuning of PI controllers. The results show the strength and ability of the technique to improve the performance of the faulty IM control.

Key words: Faulty three-phase induction motor, gravitational search algorithm, modeling, rotor field-oriented control, tuning of PI controllers

1. Introduction

Variable speed drives can provide reliable dynamic systems and important savings in the energy custom and costs of induction motors (IMs). Developing high performance control methods for IM drive systems needs an accurate motor model. Recently, various techniques of modeling induction machines have been presented [1–9]. In [1,2] dynamic mesh reluctances, in [3,4] the d-q model, in [5,6] the enhanced equivalent circuit, and in [7,8] the winding function method (WFM) have been reported for modeling induction machines. One of the most commonly models used for IMs is the d-q model [9], presented by Park. This method is based on the assumption that the stator windings are sinusoidal distributed. This supposition caused the harmonics of the windings distribution to be removed in the machine analysis. A method based on the real distribution of stator winding for modeling and calculation of mutual inductances, which is called the WFM, was proposed by Toliyat and Lipo [7,8]. One of the advantages of the WFM is the ability to model the fault conditions such as cut-out fault in IMs. In [10–14], the WFM is used to analyze some common faults in IMs such as broken rotor bars, cracked rotor end rings, shorting, opening, and abnormal stator winding circuit. Several methods have been also presented to develop detection of faults in IMs such as stator winding faults [15,16] and rotor bar faults [17,18]. One of the major failures in IMs is open-phase faults. Open-phase faults occur with the opening of windings, blown fuses, etc. Based on IM equations, in [19] with comparison between current space phasor and measured value, in [20] the extended Kalman filter (EKF) and unknown input observer, in

*Correspondence: e.alimonadi@gmail.com

[21] neural networks and look up table, and in [22] negative sequence current estimation have been shown for detection of the windings fault of stator in the motor. In [23], a small amplitude three-phase high frequency signal has been employed for detection of faults in stator windings for permanent magnet synchronous motors. This method gave fast detection of open-phase stator winding and is supposed in this work. Field-oriented control (FOC) is one of the best techniques for controlling the torque and speed in IMs. This method separates motor current into torque and flux producing components. The torque of the motor is proportional to the product of these two perpendicular components and they can be treated independently. This means that by using this method the IM control is transformed to an easy control system similar to DC motors [24]. Faulty IM control is clearly different from the balanced three-phase IM control. By using the usual balanced IM control, for faulty IMs, considerable ripples in the torque and speed response will be present [3,4]. In 1996, Zhao and Lipo presented a method for modeling and controlling of a multiphase IM based on FOC when one of the stator phases is cut off [25,26]. In addition [27] presented an approach for modeling (d-q model) and controlling (FOC method) of a dual three-phase IM when two stator phases are cut off. In [3,4], Jannati et al. showed how the conventional FOC technique can be used for faulty three-phase IM control. The authors showed that with some changes in the conventional vector control, unbalanced three-phase IM control is possible. In the process of obtaining the FOC equations however, the backward components of the stator voltage equations have been neglected [3,4]. In the present paper, d-q and WFM are discussed for modeling of a faulty IM (three-phase IM under open-phase fault). Moreover, a new method for vector control of a faulty three-phase IM based on the rotor flux oriented-control (RFOC) method is checked by simulations. In the proposed control method, two new rotational transformations are used for the equations of the faulty IM. By using these matrixes, the faulty motor equations become similar to the balanced equations. The research potential of the presented drive system for faulty motors is particularly towards the development of PI controllers. Therefore, optimization of the PI controllers for having high performance of the presented controlling method is essential. Some important optimization algorithms techniques are as follows.

Central force optimization (CFO) [28], genetic algorithm (GA) [29], artificial immune systems (AIS) [30], particle swarm optimization (PSO) [31,32], simulated annealing (SA) [33], ant colony optimization (ACO) [34], bacterial foraging algorithm (BFA) [35,36], and gravitational search algorithm (GSA) [37] are evolutionary algorithms that have been proposed for global optimization, e.g., complex nonlinear problems. These methods are increasingly analyzed or improved by researchers in different areas [38–42]. These algorithms are inspired by nature, starting from some solution points called population and determination of a global solution for problems based on nature's rules. Some efforts have been made to compare the performance of these algorithms with each other [37,43–47]. The GSA is based on the Newtonian laws of gravity and was first introduced by Rashedi et al. [37]. It models the masses that attract each other in the search space based on gravity laws, which means that a heavy mass has greater gravitational force and move slowly. Each mass is a problem solution and so a heavier mass is related to a good solution. In [37] the authors showed the GSA is more accurate and leads to greater benefits in finding a global minimum point. The presented method in [37] has been compared with some familiar heuristic search approaches such as the GA, PSO, and CFO. In this research, PI controller gains are obtained off-line by the GSA based on the speed error. The proposed method in this paper not only can be used for critical industrial applications where we need to have a fault-tolerant drive system but also can be employed for vector control of a single-phase IM (the single-phase IM can be considered an unbalanced two-phase IM). This paper is organized as follows: in part 2, the d-q model of a faulty three-phase IM with unequal stator windings is presented. The WFM model of the faulty three-phase IM is presented in part 3.

After that, the vector control equations for the faulty IM by using conventional transformations are presented in part 4. In addition, the main idea of using rotational transformations for faulty three-phase IM control and RFOC equations for the faulty motor by using novel transformations is expounded in this part. A brief overview of the GSA algorithm is presented in part 5. The simulation results are shown in part 6 and part 7 concludes the paper.

2. d-q Model for a faulty three-phase IM

The faulty IM drive can be shown as Figure 1 (assume that a phase cut-out happened in phase "c$_s$").

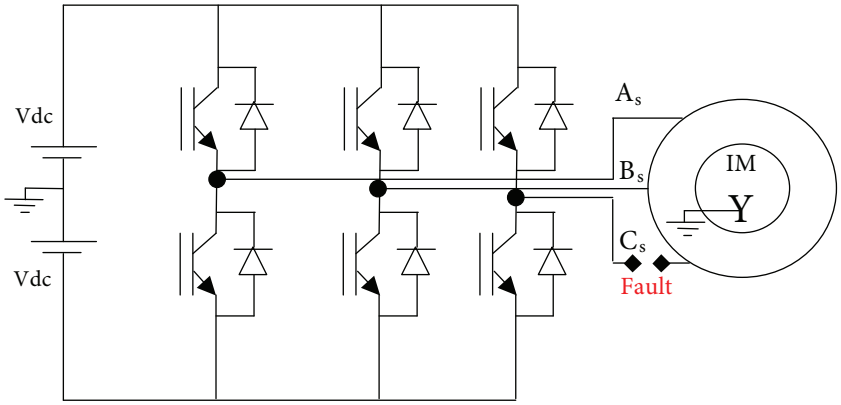

Figure 1. Faulty IM drive.

Sinusoidal waveform is considered for spatial distribution of the windings. Rotor and stator flux winding's flux axes under open-phase fault can be presented as Figure 2.

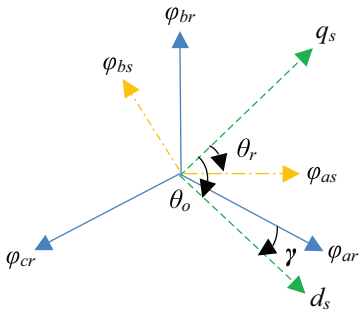

Figure 2. Rotor and stator winding's flux axes under open-phase fault.

In Figure 2, θ_r is the angle between "a$_s$" and "a$_r$" axes and θ_o is the angle between "a$_s$" and "d$_s$" axes. Based on Figure 2,

$$\gamma = \theta_o - \theta_r \tag{1}$$

According to Figure 2, the normalized transformation for the stator and rotor components is obtained as [4]

$$[T_S] = 1/\sqrt{2} \begin{bmatrix} 1 & -1 \\ 1 & 1 \end{bmatrix} \tag{2}$$

$$[T_r] = \sqrt{2/3} \begin{bmatrix} \cos(\gamma) & \cos(\gamma + 2\pi/3) & \cos(\gamma + 4\pi/3) \\ \sin(\gamma) & \sin(\gamma + 2\pi/3) & \sin(\gamma + 4\pi/3) \end{bmatrix} \tag{3}$$

Applying the transformation vectors ($[T_S]$ and $[T_r]$), the d-q model for the faulty motor in the stator reference frame (superscript "s") is obtained as follows (see Appendix A):

$$v_{ds}^s = r_{ds} i_{ds}^s + \frac{d\lambda_{ds}^s}{dt}, v_{qs}^s = r_{qs} i_{qs}^s + \frac{d\lambda_{qs}^s}{dt} \tag{4}$$

$$0 = r_r i_{dr}^s + \frac{d\lambda_{dr}^s}{dt} + \omega_r \lambda_{qr}^s, 0 = r_r i_{qr}^s + \frac{d\lambda_{qr}^s}{dt} - \omega_r \lambda_{dr}^s \tag{5}$$

$$\lambda_{ds}^s = L_{ds} i_{ds}^s + M_d i_{dr}^s, \lambda_{qs}^s = L_{qs} i_{qs}^s + M_q i_{qr}^s \tag{6}$$

$$\lambda_{dr}^s = M_d i_{ds}^s + L_r i_{dr}^s, \lambda_{qr}^s = M_q i_{qs}^s + L_r i_{qr}^s \tag{7}$$

$$\tau_e = \frac{Pole}{2}(M_q i_{qs}^s i_{dr}^s - M_d i_{ds}^s i_{qr}^s) \tag{8}$$

$$\frac{Pole}{2}(\tau_e - \tau_l) = J\frac{d\omega_r}{dt} + F\omega_r, \tag{9}$$

where v_{ds}^s and v_{qs}^s are the d-q axes voltages, i_{ds}^s and i_{qs}^s are the stator d-q axes currents i_{dr}^s and i_{qr}^s are the rotor d-q axes currents, λ_{ds}^s and λ_{qs}^s are the stator d-q axes fluxes, and λ_{dr}^s and λ_{qr}^s are the rotor d-q axes fluxes. r_{ds}, r_{qs}, and r_r indicate the stator and rotor resistances. L_{ds}, L_{qs}, M_d, M_q, and L_r indicate the stator and rotor self and mutual inductances. τ_e, τ_l, J, and F are electromagnetic torque, load torque, inertia, and viscous friction coefficient and ω_r is the motor speed. As can be seen from Eqs. (4)–(9), the equations of the three-phase IM under open-phase fault have the same structure fault with the equations of the balanced three-phase IM. Actually, by substituting $r_{ds} = r_{qs} = r_s$, $L_{ds} = L_{qs} = L_s$ and $M_d = M_q = M$ in the equations of the faulty motor, we can obtain the familiar equations of balanced motor. For a three-phase IM with balanced stator windings in the faulty mode, we have [4]

$$r_s = r_{ds} = r_{qs}, L_{ds} = L_{ls} + 1.5L_{ms}$$
$$L_{qs} = L_{ls} + 0.5L_{ms}, M_d = 1.5L_{ms}$$
$$M_q = \sqrt{3}/2 L_{ms}, L_r = L_{lr} + 1.5L_{ms}$$

In summary, the difference between the d-q model of the balanced and faulty three-phase IM equations are summarized in Table 1.

Table 1. Comparison between d-q model of the balanced and faulty three-phase IM equations.

Balanced motor	Faulty motor
q-axis mutual inductance as follows: $M = \frac{3}{2}L_{ms}$	q-axis mutual inductance as follows: $M_q = \frac{\sqrt{3}}{2}L_{ms}$
stator q-axis self inductance as follows: $L_s = L_{ls} + \frac{3}{2}L_{ms}$	stator q-axis self inductance as follows: $L_{qs} = L_{ls} + \frac{1}{2}L_{ms}$

3. WFM model for the faulty three-phase IM

An alternative method that can be used to model IMs is by using the WFM. In this method, the actual spatial distribution of windings is considered. In the analysis using the WFM, the following assumptions are normally applied:

- Uniform air gap
- Same rotor bars
- Skew effect is neglected
- Saturation is negligible

The equations of a balanced three-phase IM with "m" rotor bars can be written as follows [7,8]:

$$\begin{array}{lll} V_s = R_s I_s + \frac{d}{dt}\Lambda_s & , & \Lambda_s = L_{ss} I_s + L_{sr} I_r \quad , \quad \omega_r = \frac{d\theta_r}{dt} \\ V_r = R_r I_r + \frac{d}{dt}\Lambda_r & , & \Lambda_r = L_{rr} I_r + L_{sr}^T I_s \quad , \quad T_e = I_s^T \frac{\partial L_{sr}}{\partial \theta_r} I_r \end{array} \tag{10}$$

where

$$\begin{aligned} V_s &= \left[\begin{array}{ccc} v_1^s & v_2^s & v_3^s \end{array} \right]^T \quad , \quad I_s = \left[\begin{array}{ccc} i_1^s & i_2^s & i_3^s \end{array} \right]^T \\ \Lambda_s &= \left[\begin{array}{ccc} \Lambda_1^s & \Lambda_2^s & \Lambda_3^s \end{array} \right]^T \quad , \quad I_r = \left[\begin{array}{cccc} i_1^r & i_2^r & \ldots & i_m^r \end{array} \right]^T \\ V_r &= \left[\begin{array}{cccc} v_1^r & v_1^r & \ldots & v_m^r \end{array} \right]^T = \left[\begin{array}{cccc} 0 & 0 & \ldots & 0 \end{array} \right]^T \end{aligned}$$

R_s, R_r, L_{ss}, L_{rr}, and L_{sr} are defined in Appendix A. The motor that is investigated in this paper has 28 rotor bars and 36 stator slots. Figures 3 and 4 show the turn function for the stator phases and the first rotor bar for the simulated balanced motor, respectively (for the second rotor bar, the waveform of Figure 4 is shifted to the right by $2\pi/28 = \pi/14$). In the WFM, the winding function is defined as $N(\varphi) = n(\varphi) - < n(\varphi) >$, where $n(\varphi)$ is the turn function and $< n(\varphi) >$ is the average value of the turn function. Therefore, based on Figures 3 and 4, the winding functions of the stator phases and the first rotor bar are shown in Figures 5 and 6, respectively. The mutual inductance between windings "B" and "A" (L_{BA}) in terms of turn function and winding function is calculated by the following equation [7]:

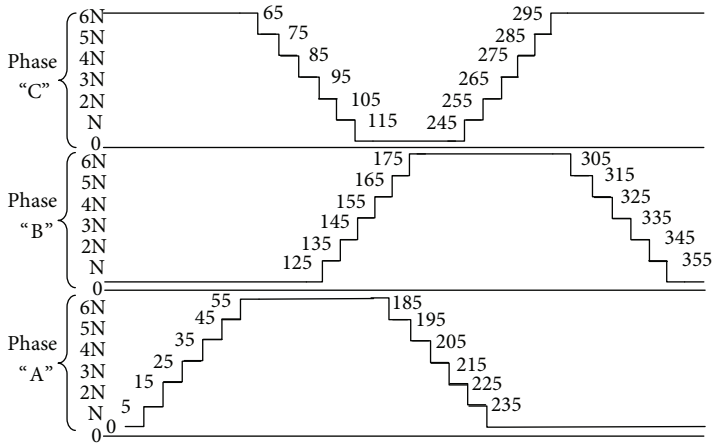

Figure 3. Turn function of stator phases for simulated motor.

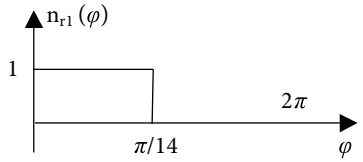

Figure 4. Turn function of the first rotor bar for simulated motor.

$$L_{BA}(\theta_{rm}) = \mu_o r \left(\int_0^{2\pi} \int_0^{l} n_B(\phi, z, \theta_{rm})\, N_A(\phi, z, \theta_{rm})\; g^{-1}(\phi, z, \theta_{rm})\, dz d\phi \right), \tag{11}$$

where "r" is the average radius of the air gap, "l" is the length of tack, "g" is the air gap function, "n_B" is the turn function of the winding "B", and "N_A" is the winding function of the winding "A". From Figures 2–5 and Eq. (11), L_{ss}, L_{sr}, and L_{rr} can be calculated for the balanced three-phase IM. Eq. (10) can be written as

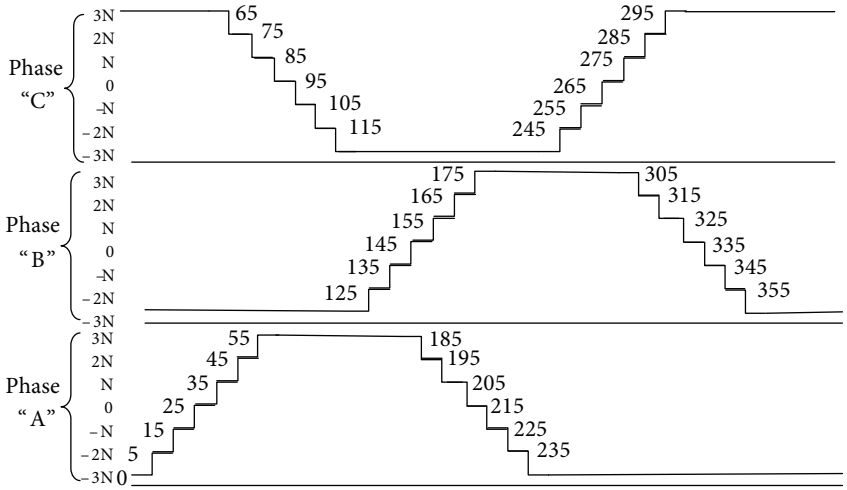

Figure 5. Winding function of stator phases for simulated motor.

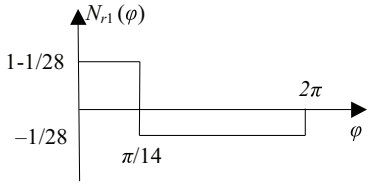

Figure 6. Winding function of the first rotor bar for simulated motor.

$$\begin{bmatrix} v_1^s - v_2^s \\ v_2^s - v_3^s \end{bmatrix} = \begin{bmatrix} v_{12}^s \\ v_{23}^s \end{bmatrix} = \begin{bmatrix} r_s & -r_s & 0 \\ 0 & r_s & -r_s \end{bmatrix} \begin{bmatrix} i_1^s \\ i_2^s \\ i_3^s \end{bmatrix} + \frac{d}{dt} \begin{bmatrix} \Lambda_1^s - \Lambda_2^s \\ \Lambda_2^s - \Lambda_3^s \end{bmatrix}, \tag{12}$$

where

$$\begin{bmatrix} \Lambda_1^s - \Lambda_2^s \\ \Lambda_2^s - \Lambda_3^s \\ 0 \end{bmatrix} = \begin{bmatrix} L_{11}^s - L_{21}^s & L_{12}^s - L_{22}^s & L_{13}^s - L_{23}^s \\ L_{21}^s - L_{31}^s & L_{22}^s - L_{32}^s & L_{23}^s - L_{33}^s \\ 1 & 1 & 1 \end{bmatrix} \begin{bmatrix} i_1^s \\ i_2^s \\ i_3^s \end{bmatrix} + \begin{bmatrix} L_{11}^{sr} - L_{21}^{sr} & L_{12}^{sr} - L_{22}^{sr} & \dots & L_{128}^{sr} - L_{228}^{sr} \\ L_{21}^{sr} - L_{31}^{sr} & L_{22}^{sr} - L_{32}^{sr} & \dots & L_{228}^{sr} - L_{328}^{sr} \\ 0 & 0 & \dots & 0 \end{bmatrix} \begin{bmatrix} i_1^r \\ i_2^r \\ \vdots \\ i_{28}^r \end{bmatrix}$$

Equations of the faulty motor have the same formation as the balanced motor equations. The only difference is that, in the faulty mode, the row and column for the phase "c $_s$" are eliminated.

4. RFOC for the faulty three-phase IM

In the RFOC method, by using the following matrix, machine equations are transferred to the rotating reference frame [24]:

$$[T_s^e] = \begin{bmatrix} \cos\theta_e & \sin\theta_e \\ -\sin\theta_e & \cos\theta_e \end{bmatrix}, \tag{13}$$

where θ_e is the angle between the stationary reference frame and rotating reference frame. By applying conventional transformation to the faulty motor (Eqs. (4)–(9)), the following equations are obtained:

Stator d-axis voltage equation:

$$\begin{aligned} v_{ds}^{+e} &= (\tfrac{r_{ds}+r_{qs}}{2})i_{ds}^{+e} + (\tfrac{L_{ds}+L_{qs}}{2})\tfrac{di_{ds}^{+e}}{dt} - \omega_e(\tfrac{L_{ds}+L_{qs}}{2})i_{qs}^{+e} + (\tfrac{M_d+M_q}{2})\tfrac{di_{dr}^{+e}}{dt} \\ &\quad -\omega_e(\tfrac{M_d+M_q}{2})i_{qr}^{+e} + (\tfrac{r_{ds}-r_{qs}}{2})i_{ds}^{-e} + (\tfrac{L_{ds}-L_{qs}}{2})\tfrac{di_{ds}^{-e}}{dt} + \omega_e(\tfrac{L_{ds}-L_{qs}}{2})i_{qs}^{-e}(\tfrac{M_d-M_q}{2})\tfrac{di_{dr}^{-e}}{dt} \\ &\quad +\omega_e(\tfrac{M_d-M_q}{2})i_{qr}^{-e} \end{aligned} \tag{14}$$

Stator q-axis voltage equation:

$$\begin{aligned} v_{qs}^{+e} &= (\tfrac{r_{ds}+r_{qs}}{2})i_{qs}^{+e} + (\tfrac{L_{ds}+L_{qs}}{2})\tfrac{di_{qs}^{+e}}{dt} + \omega_e(\tfrac{L_{ds}+L_{qs}}{2})i_{ds}^{+e} + \omega_e(\tfrac{M_d+M_q}{2})i_{dr}^{+e} \\ &\quad +(\tfrac{M_d+M_q}{2})\tfrac{di_{qr}^{+e}}{dt} - (\tfrac{r_{ds}-r_{qs}}{2})i_{qs}^{-e} - (\tfrac{L_{ds}-L_{qs}}{2})\tfrac{di_{qs}^{-e}}{dt} + \omega_e(\tfrac{L_{ds}-L_{qs}}{2})i_{ds}^{-e} \\ &\quad +\omega_e(\tfrac{M_d-M_q}{2})i_{dr}^{-e} - (\tfrac{M_d-M_q}{2})\tfrac{di_{qr}^{-e}}{dt} \end{aligned} \tag{15}$$

Rotor d-axis voltage equation:

$$\begin{aligned} 0 &= (\tfrac{M_d+M_q}{2})\tfrac{di_{ds}^{+e}}{dt} - (\omega_e-\omega_r)(\tfrac{M_d+M_q}{2})i_{qs}^{+e} + r_r i_{dr}^{+e} + L_r\tfrac{di_{dr}^{+e}}{dt} - (\omega_e-\omega_r)L_r i_{qr}^{+e} \\ &\quad +(\tfrac{M_d-M_q}{2})\tfrac{di_{ds}^{-e}}{dt} + (\omega_e-\omega_r)(\tfrac{M_d-M_q}{2})i_{qs}^{-e} \end{aligned} \tag{16}$$

Rotor q-axis voltage equation:

$$\begin{aligned} 0 &= (\tfrac{M_d+M_q}{2})\tfrac{di_{qs}^{+e}}{dt} + (\omega_e-\omega_r)(\tfrac{M_d+M_q}{2})i_{ds}^{+e} + r_r i_{qr}^{+e} + L_r\tfrac{di_{qr}^{+e}}{dt} + (\omega_e-\omega_r)L_r i_{dr}^{+e} \\ &\quad -(\tfrac{M_d-M_q}{2})\tfrac{di_{qs}^{-e}}{dt} + (\omega_e-\omega_r)(\tfrac{M_d-M_q}{2})i_{ds}^{-e} \end{aligned} \tag{17}$$

where

$$\begin{bmatrix} i^{+e}_{ds,dr} \\ i^{+e}_{qs,qr} \end{bmatrix} = \begin{bmatrix} \cos\theta_e & \sin\theta_e \\ -\sin\theta_e & \cos\theta_e \end{bmatrix} \begin{bmatrix} i^{s}_{ds,dr} \\ i^{s}_{qs,qr} \end{bmatrix}$$
$$\begin{bmatrix} i^{-e}_{ds,dr} \\ i^{-e}_{qs,qr} \end{bmatrix} = \begin{bmatrix} \cos\theta_e & -\sin\theta_e \\ \sin\theta_e & \cos\theta_e \end{bmatrix} \begin{bmatrix} i^{s}_{ds,dr} \\ i^{s}_{qs,qr} \end{bmatrix}$$

In general, Eqs. (14)–(17) include two terms, "$+e$": forward components and "$-e$": backward components as shown in Figure 7. Each of these terms (forward or backward terms) is like a balanced motor that turns in the forward or backward direction (in the equations of balanced IM, there are no backward terms). The faulty IM control can be done by controlling forward and backward components independently but the control scheme will be very complex. The backward components are generated because of different inductances in the faulty IM model equations ($M_d \neq M_q$ and $L_{ds} \neq L_{qs}$). In this paper, rotational transformations for the stator variables that resolve this problem are proposed. The main idea of this transformation is obtained from the steady-state equivalent circuit of the single-phase IM. This motor is generally unbalanced with two unequal main and auxiliary windings, which are displaced from each other by 90°. The equivalent circuit of a single-phase IM is shown in Figure 8 [48]. All the parameters in Figure 8 are defined in [48]. By applying equation (18), a simplified circuit can be shown as Figure 9.

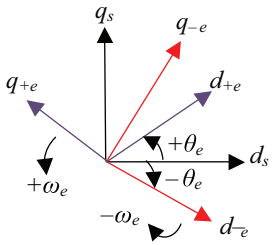

Figure 7. Forward, backward, and stationary reference frame.

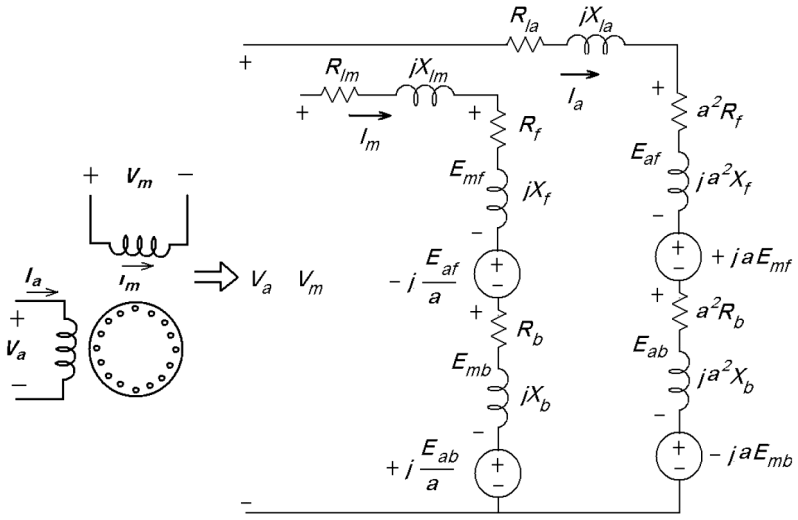

Figure 8. Single-phase IM equivalent circuit.

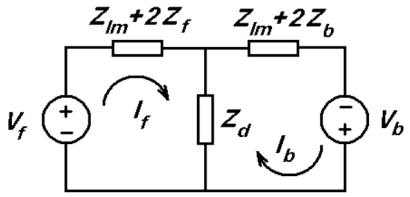

Figure 9. Simplified single-phase IM equivalent circuit.

$$\begin{aligned} V_f &= \tfrac{1}{2}\left(V_m - j\tfrac{V_a}{a}\right) \ , \ V_b = \tfrac{1}{2}\left(V_m + j\tfrac{V_a}{a}\right) \\ I_f &= \tfrac{1}{2}\left(I_m - jaI_a\right) \ , \ I_b = \tfrac{1}{2}\left(I_m + jaI_a\right) \end{aligned} \tag{18}$$

From Figure 9,

$$Z_d = \frac{1}{2}\left(\frac{Z_{la}}{a^2} - Z_{lm}\right) \tag{19}$$

Based on Figure 9, if we ignore Z_d, this figure can be changed into a balanced circuit. In this case, jI_f, I_f and jV_f, V_f are the currents and voltages of the balanced IM. Eq. (18), with neglecting of Z_d, can be rewritten as

$$\begin{bmatrix} jV_f \\ V_f \end{bmatrix} = \begin{bmatrix} \frac{1}{a} & j \\ -j\frac{1}{a} & 1 \end{bmatrix} \begin{bmatrix} V_a \\ V_m \end{bmatrix}, \begin{bmatrix} jI_f \\ I_b \end{bmatrix} = \begin{bmatrix} a & j \\ -ja & 1 \end{bmatrix} \begin{bmatrix} I_a \\ I_m \end{bmatrix} \tag{20}$$

Eq. (20) indicates transformation matrixes for changing the variables from unbalanced mode to balanced mode (e.g., V_a and V_m to V_f and jV_f). From Eq. (20):

Proposed rotational transformation for stator voltages:

$$\begin{bmatrix} \nu_{ds}^e \\ \nu_{qs}^e \end{bmatrix} = [T_{vs}^e] \begin{bmatrix} \nu_{ds}^s \\ \nu_{qs}^s \end{bmatrix} = \begin{bmatrix} \sqrt{\frac{L_{qs}}{L_{ds}}}\cos\theta_e & \sin\theta_e \\ -\sqrt{\frac{L_{qs}}{L_{ds}}}\sin\theta_e & \cos\theta_e \end{bmatrix} \begin{bmatrix} \nu_{ds}^s \\ \nu_{qs}^s \end{bmatrix} \tag{21}$$

Proposed rotational transformation for stator currents:

$$\begin{bmatrix} i_{ds}^e \\ i_{qs}^e \end{bmatrix} = [T_{is}^e] \begin{bmatrix} i_{ds}^s \\ i_{qs}^s \end{bmatrix} = \begin{bmatrix} \sqrt{\frac{L_{ds}}{L_{qs}}}\cos\theta_e & \sin\theta_e \\ -\sqrt{\frac{L_{ds}}{L_{qs}}}\sin\theta_e & \cos\theta_e \end{bmatrix} \begin{bmatrix} i_{ds}^s \\ i_{qs}^s \end{bmatrix} \tag{22}$$

In our deduction the following substitutions are used:

$$\begin{aligned} &1 \to \cos\theta_e, j \to \sin\theta_e, \tfrac{1}{a} = \tfrac{N_m}{N_a} \to \tfrac{N_q}{N_d} = \sqrt{\tfrac{L_{qs}}{L_{ds}}} \\ &V_f \to v_{qs}^e, jV_f \to v_{ds}^e, V_a \to v_{ds}^s, V_m \to v_{qs}^s \\ &I_f \to i_{qs}^e, jI_f \to i_{ds}^e, I_a \to i_{ds}^s, I_m \to i_{qs}^s \end{aligned} \tag{23}$$

As is shown, by simplifying the single-phase IM equivalent circuit, two novel rotational transformations are obtained. It is expected by applying these matrixes (Eqs. (21) and (22)) to the faulty IM equations, the equations of the faulty IM become like balanced equations. By considering $L_{qs}/L_{ds} = (M_q/M_d)^2$ (in d-q

model of faulty IM: $M_d = 3/2\ L_{ms}$, $M_q = \sqrt{3}/2\ L_{ms}$, $L_{ds} = L_{ls} + 3/2\ L_{ms}$, $L_{qs} = L_{ls} + 1/2\ L_{ms}$ and L_{ms} ?? L_{ls}), which is equivalent to neglecting inductance of Z_d in Figure 9, rotor voltages, flux, and torque equations become like balanced IM equations (the only difference is that in the balanced mode we have $M = 3/2\ L_{ms}$ and in the faulty mode we have $M_q = \sqrt{3}/2\ L_{ms}$). However, the equations of stator voltage include forward terms and backward terms (equations of flux, torque, rotor voltage, and stator voltage without supposition of $L_{qs}/L_{ds} = (M_q/M_d)^2$ are given in Appendix B).

In the RFOC method [24]:

$$\lambda_{dr}^e = |\lambda_r| \quad , \quad \lambda_{qr}^e = 0 \tag{24}$$

Consequently, RFOC equations for the faulty IM are gained as

$$\begin{aligned}
&|\lambda_r| = \tfrac{M_q i_{ds}^e}{1+T_r d/dt} \\
&\omega_e = \omega_r + \tfrac{M_q i_{qs}^e}{T_r |\lambda_r|} \\
&\tau_e = \tfrac{pole}{2} \tfrac{M_q}{L_r} |\lambda_r| \, i_{qs}^e \\
&v_{ds}^e = v_{ds}^d + v_{ds}^{ref} + v_{ds}^{-e} \\
&v_{qs}^e = v_{qs}^d + v_{qs}^{ref} + v_{qs}^{-e}
\end{aligned} \tag{25}$$

where

$$\begin{aligned}
&v_{ds}^d = -\omega_e i_{qs}^e (L_{qs} - \tfrac{M_q^2}{L_r}) + (\tfrac{M_q}{L_r})(\tfrac{M_q i_{ds}^e - |\lambda_r|}{T_r}) \\
&v_{ds}^{ref} = (\tfrac{r_{ds} M_q^2 + r_{qs} M_d^2}{2 M_d^2}) i_{ds}^e + (L_{qs} - \tfrac{M_q^2}{L_r}) \tfrac{d i_{ds}^e}{dt} \\
&v_{qs}^d = \omega_e i_{ds}^e (L_{qs} - \tfrac{M_q^2}{L_r}) + \omega_e M_q \tfrac{|\lambda_r|}{L_r} \\
&v_{qs}^{ref} = (\tfrac{r_{ds} M_q^2 + r_{qs} M_d^2}{2 M_d^2}) i_{qs}^e + (L_{qs} - \tfrac{M_q^2}{L_r}) \tfrac{d i_{qs}^e}{dt} \\
&\begin{bmatrix} v_{ds}^{-e} \\ v_{qs}^{-e} \end{bmatrix} = (\tfrac{r_{ds} M_q^2 - r_{qs} M_d^2}{2 M_d^2}) \begin{bmatrix} \cos 2\theta_e & -\sin 2\theta_e \\ -\sin 2\theta_e & -\cos 2\theta_e \end{bmatrix} \begin{bmatrix} i_{ds}^e \\ i_{qs}^e \end{bmatrix}
\end{aligned}$$

In Eq. (25), $T_r (T_r = L_r/r_r)$ is the rotor time constant. Moreover, v_{ds}^d and v_{qs}^d are generated using a decoupling circuit and v_{ds}^{ref} and v_{qs}^{ref} are generated using a PI controller in the vector control block diagram of the faulty IM. The comparison between stator voltage equations of the conventional RFOC and modified RFOC is summarized in Table 2. Based on Eqs. (25) and Table 2, the only difference between equations of conventional RFOC and modified RFOC is that in the modified RFOC equations it is obtained $r_s = ((M_q^2 + M_d^2)/2\ M_d^2) r_s) = 2/3\ r_s$; $M = M_q = \sqrt{3}/2\ L_{ms}$; $L_s = L_{qs} = L_{ls} + 1/2\ L_{ms}$; v_{ds}^{-e} and v_{qs}^e as above but in the conventional RFOC equations, we have r_s; $M = 3/2\ L_{ms}$; $L_s = L_{ls} + 3/2\ L_{ms}$). Therefore, Figure 10 can be recommended for the RFOC of the faulty IM. In Figure 10, the red colors illustrate the sections of the conventional controller that need to be changed for faulty motor control.

Table 2. Comparison between stator voltage equations of conventional RFOC and modified RFOC.

Conventional RFOC	Modified RFOC
Stator d-axis voltage equations [24]: $v_{ds}^e = r_s i_{ds}^e + (L_s - \frac{M^2}{L_r})\frac{di_{ds}^e}{dt}$ $-\omega_e(L_s - \frac{M^2}{L_r})i_{qs}^e + (\frac{M}{L_r})(\frac{Mi_{ds}^e - \lvert\lambda_r\rvert}{T_r})$	Stator d-axis voltage equations according to Eq. (25): $v_{ds}^e = (\frac{r_s M_q^2 + r_s M_d^2}{2M_d^2})i_{ds}^e + (L_{qs} - \frac{M_q^2}{L_r})\frac{di_{ds}^e}{dt}$ $-\omega_e(L_{qs} - \frac{M_q^2}{L_r})i_{qs}^e + (\frac{M_q}{L_r})(\frac{M_q i_{ds}^e - \lvert\lambda_r\rvert}{T_r})$ $+(\frac{r_s M_q^2 - r_s M_d^2}{2M_d^2}) \times (\cos 2\theta_e i_{ds}^e - \sin 2\theta_e i_{qs}^e)$
Stator q-axis voltage equations [24]: $v_{qs}^e = r_s i_{qs}^e + (L_s - \frac{M^2}{L_r})\frac{di_{qs}^e}{dt}$ $+\omega_e(L_s - \frac{M^2}{L_r})i_{ds}^e + \omega_e M\frac{\lvert\lambda_r\rvert}{L_r}$	Stator q-axis voltage equations according to Eq. (25): $v_{qs}^e = (\frac{r_s M_q^2 + r_s M_d^2}{2M_d^2})i_{qs}^e + (L_{qs} - \frac{M_q^2}{L_r})\frac{di_{qs}^e}{dt}$ $+\omega_e(L_{qs} - \frac{M_q^2}{L_r})i_{ds}^e + \omega_e M_q\frac{\lvert\lambda_r\rvert}{L_r}$ $+(\frac{r_s M_q^2 - r_s M_d^2}{2M_d^2}) \times (-\sin 2\theta_e i_{ds}^e - \cos 2\theta_e i_{qs}^e)$

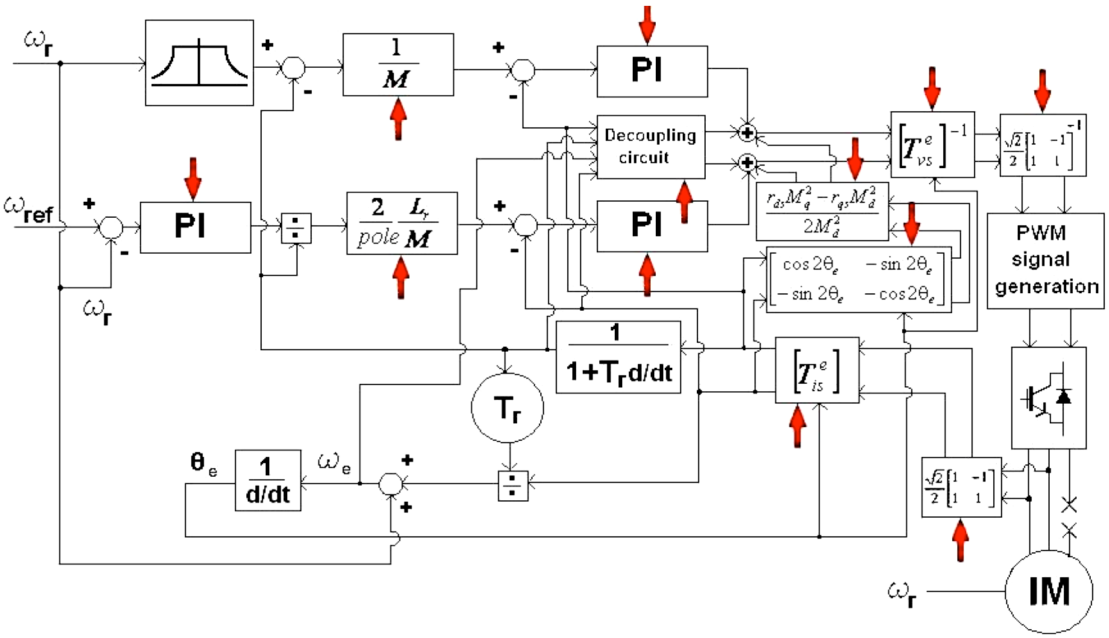

Figure 10. Proposed block diagram for faulty IM.

In conclusion, the comparison between the two vector control techniques is summarized in Table 3.

5. GSA

It can be observed that in the modified block diagram for the RFOC of the faulty three-phase IM, the PI controllers should be changed from the balanced mode to the unbalanced mode. In this paper, the GSA is employed for optimization of the PI controllers. The GSA starts with position of masses (agents) given by Eq. (26):

$$X_i = \left(x_i^1, ..., x_i^d, ..., x_i^n\right) \qquad for \;\; i = 1, 2, \ldots, N, \tag{26}$$

Table 3. Comparison between two vector control methods.

Conventional vector control for the balanced motor	Proposed modified vector control for the unbalanced motor
3 to 2 transformation for the stator currents [24]: $\begin{bmatrix} i_{ds}^s \\ i_{qs}^s \end{bmatrix} = \sqrt{\frac{2}{3}} \begin{bmatrix} +1 & -\frac{1}{2} & -\frac{1}{2} \\ 0 & \frac{\sqrt{3}}{2} & -\frac{\sqrt{3}}{2} \end{bmatrix} \begin{bmatrix} i_{as} \\ i_{bs} \\ i_{cs} \end{bmatrix}$	2 to 2 transformation for the stator currents according to Eq. (2): $\begin{bmatrix} i_{ds}^s \\ i_{qs}^s \end{bmatrix} = \underbrace{\frac{\sqrt{2}}{2} \begin{bmatrix} 1 & -1 \\ 1 & 1 \end{bmatrix}}_{[T_S]} \begin{bmatrix} i_{as} \\ i_{bs} \end{bmatrix}$
Stator resistance [24]: r_s	Stator resistance according to Eq. (25): $r_s = \frac{r_{ds}M_q^2 + r_{qs}M_d^2}{2M_d^2} = \frac{2}{3}r_s$
Stator self inductance [24]: $L_s = L_{ls} + \frac{3}{2}L_{ms}$	Stator self inductance according to Eq. (25): $L_s = L_{qs} = L_{ls} + \frac{1}{2}L_{ms}$
Stator and rotor mutual inductance [24]: $M = \frac{3}{2}L_{ms}$	Stator and rotor mutual inductance according to Eq. (25): $M = M_q = \frac{\sqrt{3}}{2}L_{ms}$
Balanced rotational transformation for the stator currents [24]: $\begin{bmatrix} i_{ds}^e \\ i_{qs}^e \end{bmatrix} = \begin{bmatrix} \cos\theta_e & \sin\theta_e \\ -\sin\theta_e & \cos\theta_e \end{bmatrix} \begin{bmatrix} i_{ds}^s \\ i_{qs}^s \end{bmatrix}$	Unbalanced rotational transformation for the stator currents according to Eq. (22): $\begin{bmatrix} i_{ds}^e \\ i_{qs}^e \end{bmatrix} = \underbrace{\begin{bmatrix} \sqrt{\frac{L_{ds}}{L_{qs}}}\cos\theta_e & \sin\theta_e \\ -\sqrt{\frac{L_{ds}}{L_{qs}}}\sin\theta_e & \cos\theta_e \end{bmatrix}}_{[T_{is}^e]} \begin{bmatrix} i_{ds}^s \\ i_{qs}^s \end{bmatrix}$
Inverse of balanced rotational transformation for the stator voltages [24]: $\begin{bmatrix} v_{ds}^s \\ v_{qs}^s \end{bmatrix} = \begin{bmatrix} \cos\theta_e & -\sin\theta_e \\ \sin\theta_e & \cos\theta_e \end{bmatrix} \begin{bmatrix} v_{ds}^e \\ v_{qs}^e \end{bmatrix}$	Inverse of unbalanced rotational transformation for the stator voltages according to Eq. (21): $\begin{bmatrix} v_{ds}^s \\ v_{qs}^s \end{bmatrix} = \underbrace{\begin{bmatrix} \cos\theta_e & -\sin\theta_e \\ \sqrt{\frac{L_{ds}}{L_{qs}}}\sin\theta_e & \sqrt{\frac{L_{ds}}{L_{qs}}}\cos\theta_e \end{bmatrix}}_{[T_{vs}^e]^{-1}} \begin{bmatrix} v_{ds}^e \\ v_{qs}^e \end{bmatrix}$
2 to 3 transformation for the stator voltages [24]: $\begin{bmatrix} v_{as} \\ v_{bs} \\ v_{cs} \end{bmatrix} = \sqrt{\frac{2}{3}} \begin{bmatrix} +1 & 0 \\ -\frac{1}{2} & \frac{\sqrt{3}}{2} \\ -\frac{1}{2} & -\frac{\sqrt{3}}{2} \end{bmatrix} \begin{bmatrix} v_{ds}^s \\ v_{qs}^s \end{bmatrix}$	2 to 2 transformation for the stator voltages according to Eq. (2): $\begin{bmatrix} v_{as} \\ v_{bs} \end{bmatrix} = \underbrace{\left(\frac{\sqrt{2}}{2} \begin{bmatrix} 1 & -1 \\ 1 & 1 \end{bmatrix}\right)^{-1}}_{[T_S]^{-1}} \begin{bmatrix} v_{ds}^s \\ v_{qs}^s \end{bmatrix}$
———	Backward components in the stator equations according to Eq. (25): $\begin{bmatrix} v_{ds}^{-e} \\ v_{qs}^{-e} \end{bmatrix} = (\frac{r_{ds}M_q^2 - r_{qs}M_d^2}{2M_d^2}) \begin{bmatrix} i_{ds}^{-e} \\ i_{qs}^{-e} \end{bmatrix} = -\frac{r_s}{3} \begin{bmatrix} i_{ds}^{-e} \\ i_{qs}^{-e} \end{bmatrix}$ $\begin{bmatrix} i_{ds}^{-e} \\ i_{qs}^{-e} \end{bmatrix} = \begin{bmatrix} \cos 2\theta_e & -\sin 2\theta_e \\ -\sin 2\theta_e & -\cos 2\theta_e \end{bmatrix} \begin{bmatrix} i_{ds}^e \\ i_{qs}^e \end{bmatrix}$
———	Tuning of PI controllers using GSA

where x_i^d is the position of the ith mass in the dth dimension. At the specific time t the force between mass "i" and mass "j" is defined as Eq. (27):

$$F_{ij}^d(t) = G(t)\frac{M_{pi}(t) \times M_{\alpha\, j}(t)}{(R_{ij}(t)+\varepsilon)(x_j^d(t) - x_i^d(t))}, \tag{27}$$

where M_a and M_p are the active and passive gravitational mass related to agents "i" and "j", respectively. $G(t)$ is a gravitational constant that is updated by Eq. (28), ε is a small constant, and $R_{ij}(t)$ is the Euclidian distance between "i" and "j" agents.

$$G(t) = G_o e^{-\alpha \frac{t}{T}} \tag{28}$$

In Eq. (28), G_o and α are user defined constants, T is the total number of iterations, and t is current iteration. The outcome of the total force on agent "i" in dimension d is equal to

$$F_i^d(t) = \sum_{j=1, j\neq i}^{N} rand_j F_{ij}^d(t), \tag{29}$$

where $rand_j$ is a random number in the interval [0, 1]. After each iteration, the velocity and position of each agent are updated as follows:

$$v_i^d(t+1) = rand_i \times v_i^d(t) + \alpha_i^d(t) \tag{30}$$

$$x_i^d(t+1) = x_i^d(t) + v_i^d(t+1) \tag{31}$$

The masses of the agents are updated by Eqs. (32)–(34).

$$M_{\alpha\, i} = M_{pi} = M_{ii} = M_i \qquad i = 1, 2, \ldots, N \tag{32}$$

$$m_i(t) = \frac{fit_i(t) - worst(t)}{best(t) - worst(t)} \tag{33}$$

$$M_i(t) = \frac{m_i(t)}{\sum_{j=1}^{N} m_j(t)} \tag{34}$$

$fit_i(t)$ represents the fitness value of the agent "i" at iteration t. $worst(t)$ and $best(t)$ are the worst and best solution in iteration t and can be defined for minimization as follows:

$$best(t) = \min_{j\in\{1,\ldots,N\}} fit_j(t) \tag{35}$$

$$worst(t) = \max_{j\in\{1,\ldots,N\}} fit_j(t) \tag{36}$$

During each iteration, the GSA reduces the number of agents based on fitness evaluation and finally one agent remains as the best solution of the problem. The principle of the GSA is presented in Figure 11 [37]. The performance of the proposed faulty IM drive system varies according to the PI controller coefficients and it is indicated by the value of the integral time absolute error (ITAE). The ITAE is considered an objective function. The purpose of the GSA is to minimize the objective function or maximize the fitness function (fitness function is 1/(ITAE + 1)). The parameter settings for the GSA are considered as follows:

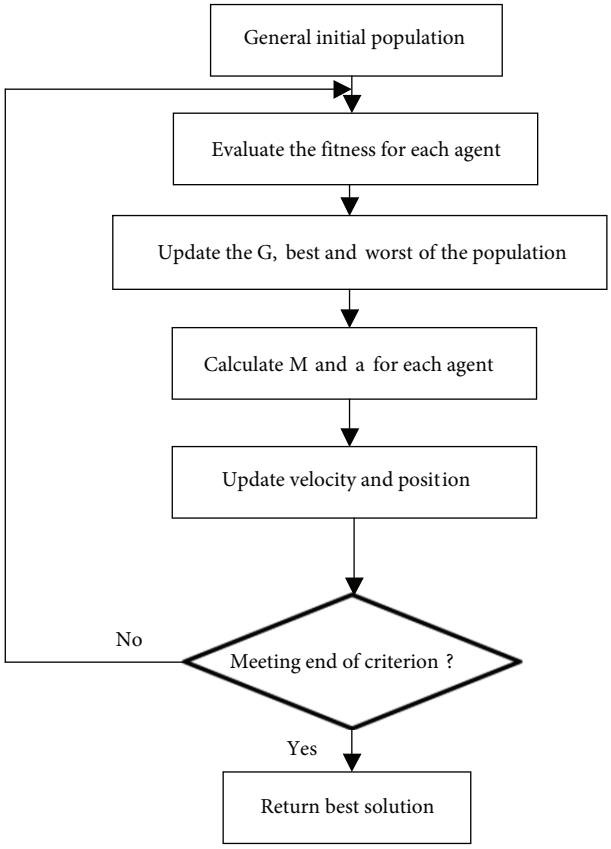

Figure 11. Principle of GSA [37].

- Population size or number of agents: 50
- Maximum iteration: 50
- In Eq. (27): $\varepsilon = 0$
- In Eq. (28): $\alpha = 20$ & $G_o = 100$ & $T = 50$

6. Simulation evaluations

To confirm the usefulness of the presented drive system for a faulty IM, a vector control drive system according to Figure 10 is simulated using MATLAB. The simulated motor is fed by a PWM, 3-leg VSI. The WFM is considered for modeling of the unbalanced motor. At the same time, the conventional RFOC is also simulated. The ratings and parameters of the motor used in the vector control are given in Appendix C.

Figures 12 and 14 show the simulation results of the conventional RFOC that is utilized even after the faulty condition is introduced. However, Figures 13 and 15 show the simulation results where the control is swapped with the one as shown in Figure 10 at the instance the fault is introduced. In Figures 12 and 13, the motor is started under healthy condition. Then a fault (cut-off in phase "c_s") is employed at t = 0.5 s. When t = 4 s, a step change in the load torque is then introduced (based on [49], the maximum permissible torque in the three-phase IM under open-phase fault is about 30% of the rated motor torque). The results demonstrate that the conventional RFOC method (Figure 12) is not capable of controlling the faulty IM accurately. However,

important decreases in the torque and speed ripples can be seen in Figure 13, after the fault is introduced. From Figure 12 it can be seen that with the conventional RFOC the time for the speed to recover to its reference value after a fault is introduced is about 2 s, whereas in Figure 13 with the proposed RFOC it only took about 0.1 s.

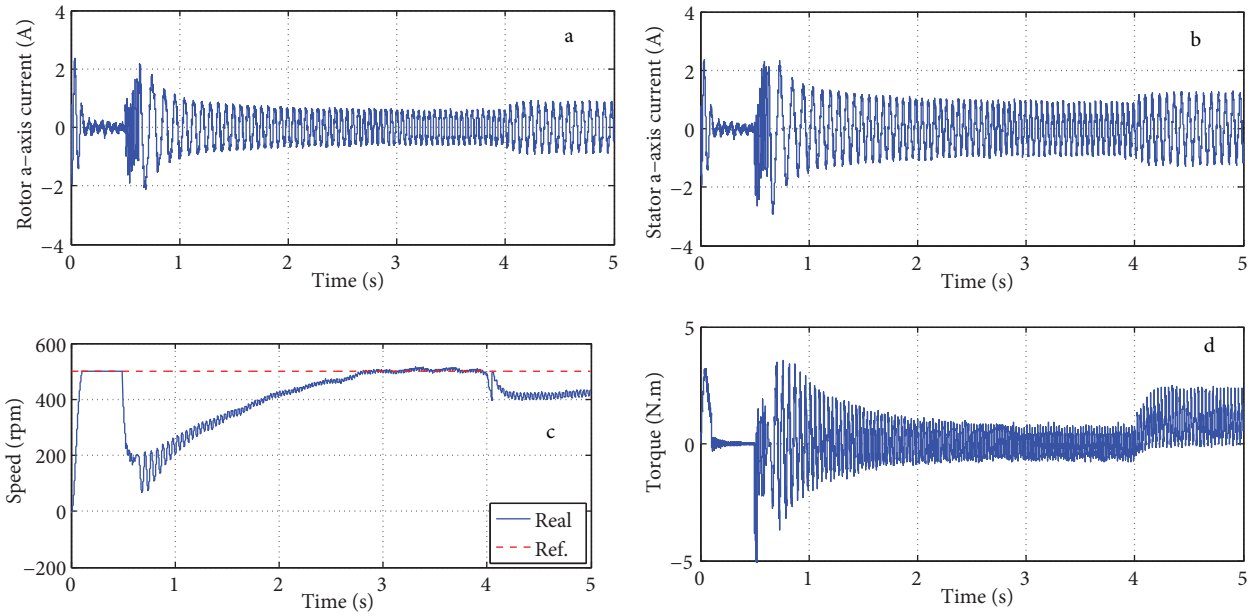

Figure 12. Simulation results of the conventional vector controller; (a) Rotor a-axis current, (b) Stator a-axis current, (c) Speed, (d) Electromagnetic torque.

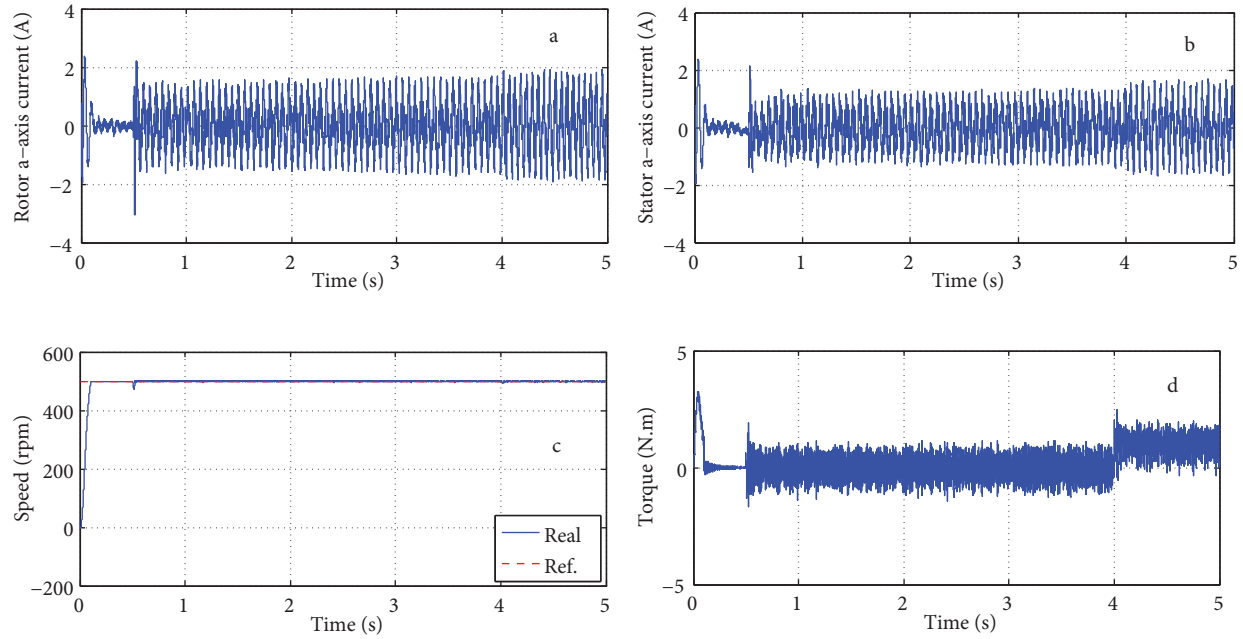

Figure 13. Simulation results of the modified vector controller; (a) Rotor a-axis current, (b) Stator a-axis current, (c) Speed, (d) Electromagnetic torque.

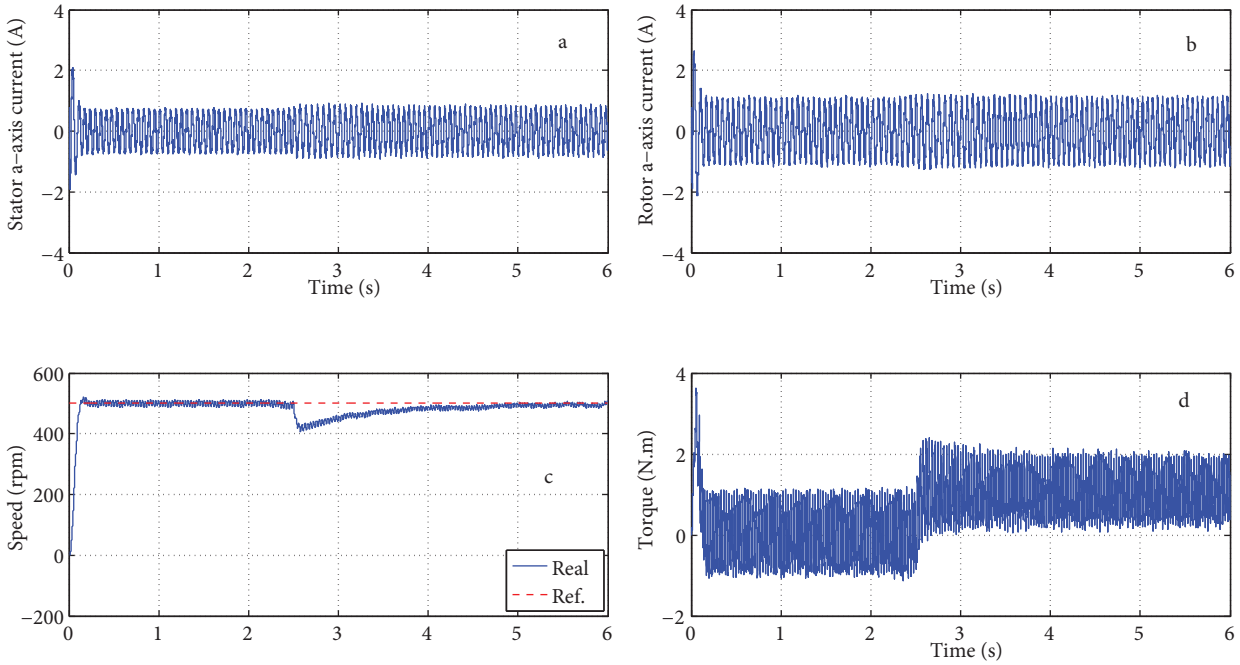

Figure 14. Simulation results of the conventional vector controller; (a) Rotor a-axis current, (b) Stator a-axis current, (c) Speed, (d) Electromagnetic torque.

In Figures 14 and 15, it is supposed that the fault happens before the motor is run (like a single-phase IM); then a load torque equal to 1 N.m at t = 2.5 s is applied to the machine. However, the proposed controller produces fewer ripples in the speed and torque with superior acceleration (in this case, as can be seen in Figure 14(c), by using the conventional controller, the speed oscillation after applying load torque and at steady state

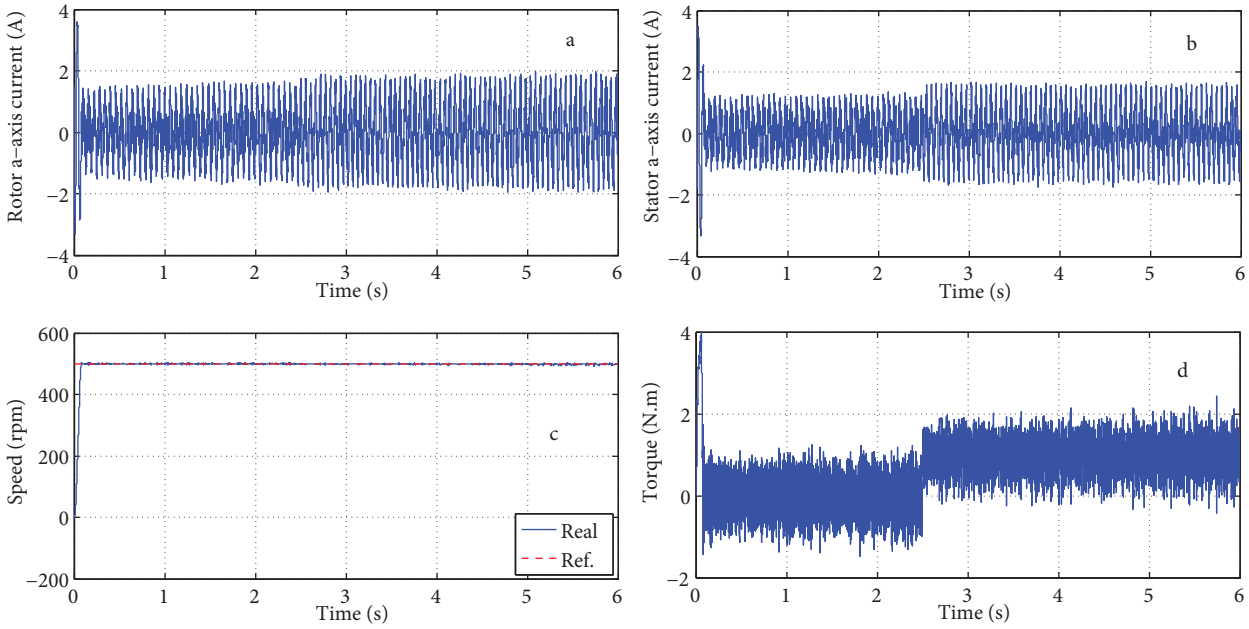

Figure 15. Simulation results of the modified vector controller; (a) Rotor a-axis current, (b) Stator a-axis current, (c) Speed, (d) Electromagnetic torque.

is $\sim$ 12 rpm at rotor speed of 500 rpm but by using the proposed modified controller (Figure 15(c)), the speed oscillation reduced notably $\sim$ 0.8 rpm at rotor speed of 500 rpm).

Figure 16 demonstrates the conventional RFOC simulated results. In starting, the IM is healthy. Then phase "c_s" of the stator is opened at t = 1 s and the IM becomes unbalanced. At the same time, a load torque equal to 0.5 N.m is applied to the machine. Simulation illustrates that the conventional RFOC is unable to control the faulty IM correctly (in this condition, the motor speed cannot reach the reference speed). Significant oscillations in the electromagnetic torque and speed on the motor are observed. In Figure 17, a similar process is performed but this time after the open-phase fault, the modified method (Figure 10) is employed. Simulation results in Figure 17 show that the proposed modified controller decreases the torque ripples noticeably.

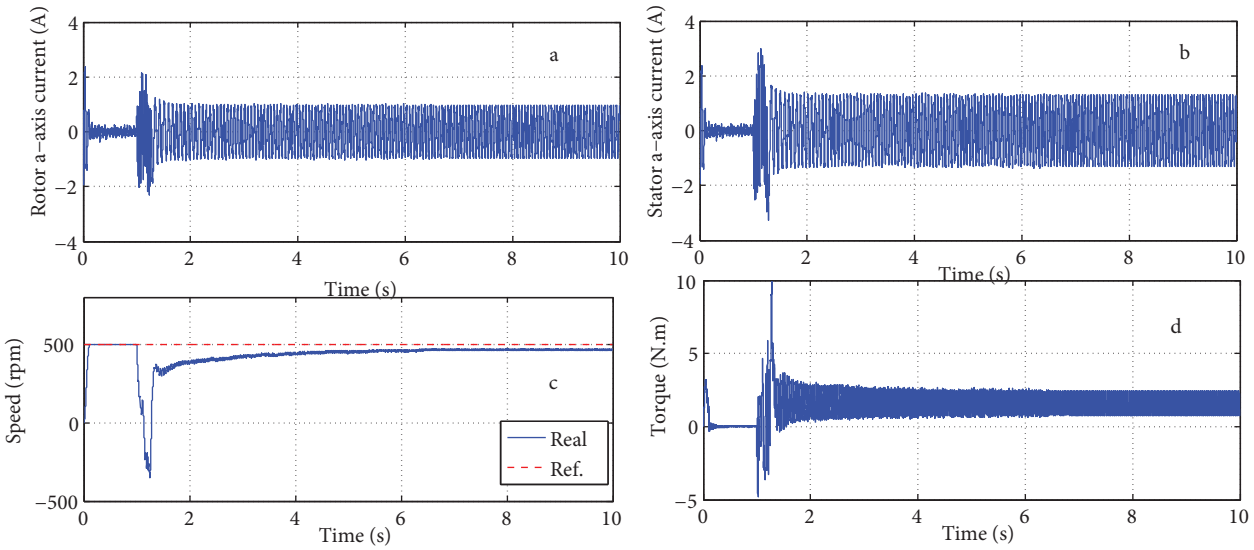

Figure 16. Simulation results of the conventional vector controller; (a) Rotor a-axis current, (b) Stator a-axis current, (c) Speed, (d) Electromagnetic torque.

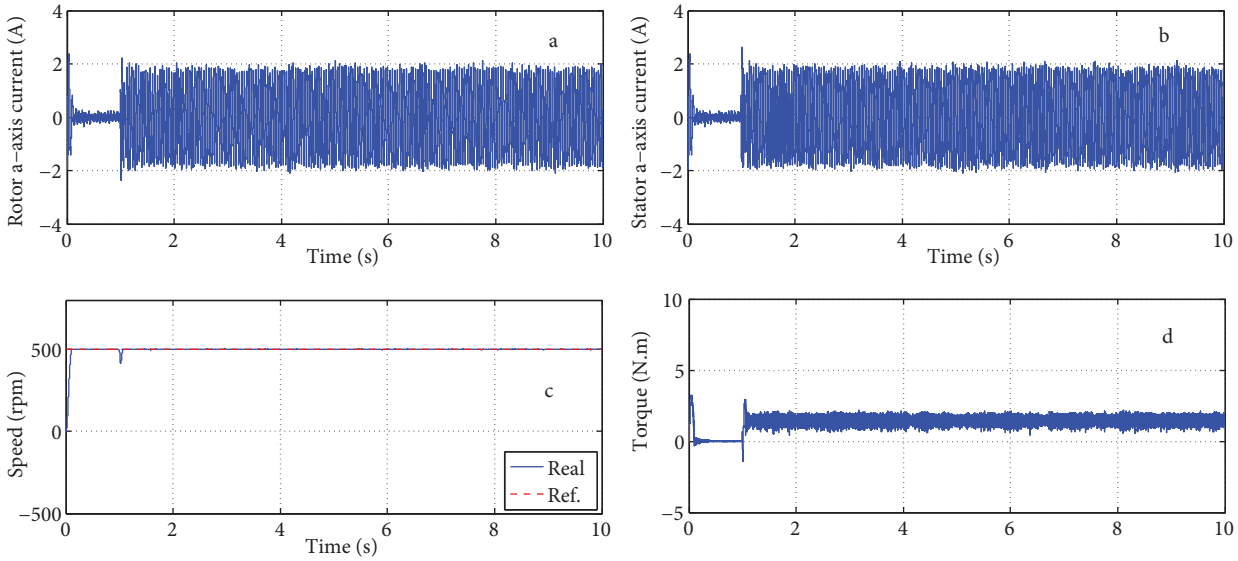

Figure 17. Simulation results of the modified vector controller; (a) Rotor a-axis current, (b) Stator a-axis current, (c) Speed, (d) Electromagnetic torque.

Figures 18 and 19 show the comparison between the conventional and modified controller (left: conventional, right: modified). In Figure 18, the motor is starting in balanced condition. Then a phase cut-off is introduced at t = 0.05 s. Moreover, a load torque equal to 0.5 Nm is applied at t = 0.4 s. In Figure 19, the motor is starting in balanced condition. Then a phase cut-off is introduced at t = 1 s. In Figure 19, two load torques equal to 0.5 Nm and 1.5 N.m are applied at t = 0.4 s and t = 3 s, respectively. Simulation results of the conventional RFO controller show that the conventional controller is unable to control the IM under open-phase fault properly (e.g., as can be seen in Figure 18, by using the conventional controller, the speed oscillation after applying load torque and at steady state is $\sim$ 8 rpm at rotor speed of 500 rpm but by using the proposed modified controller the speed oscillation reduced notably $\sim$ 0.5 rpm at rotor speed of 500 rpm. Moreover, from Figure 19 (c-left), it is observed that the real speed cannot follow the reference speed after applying load torque at t = 3 s). It can be seen from Figures 18 and 19 that the dynamic performance of the proposed system for vector control of the faulty three-phase IM is extremely acceptable.

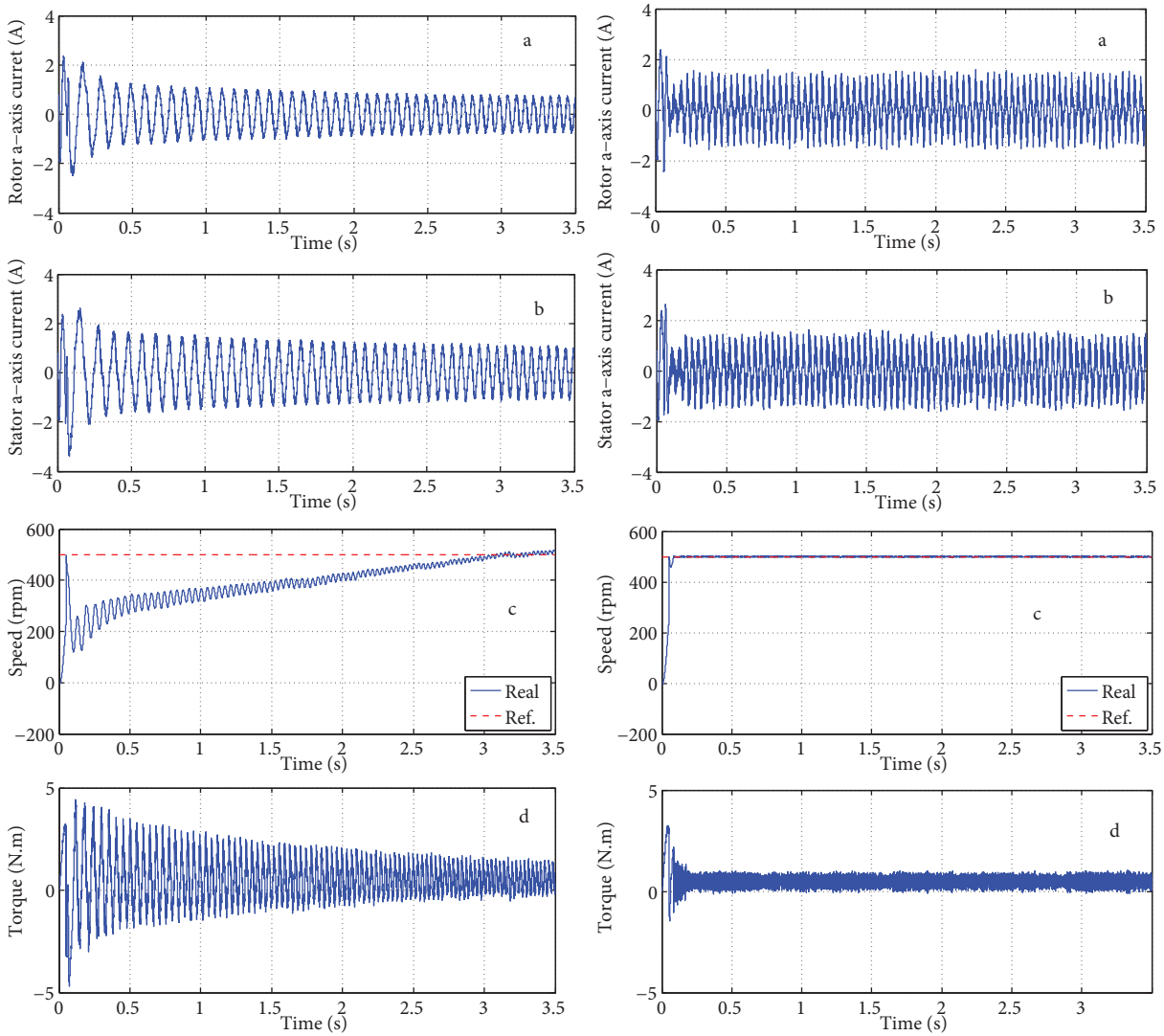

Figure 18. Simulation results of the conventional (left) and modified (right) controller; (a) Rotor a-axis current, (b) Stator a-axis current, (c) Speed, (d) Electromagnetic torque.

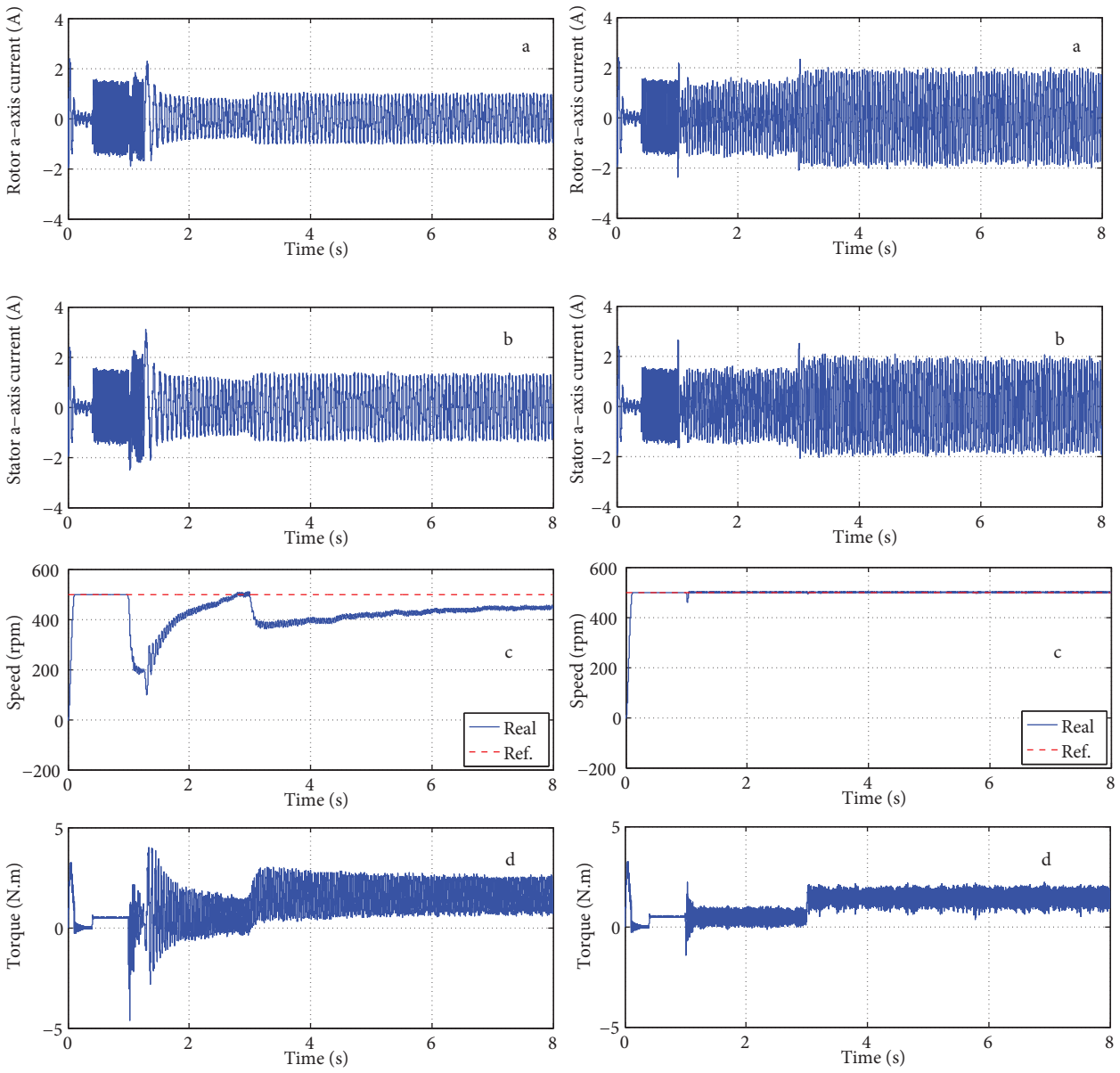

Figure 19. Simulation results of the conventional (left) and modified (right) controller; (a) Rotor a-axis current, (b) Stator a-axis current, (c) Speed, (d) Electromagnetic torque.

Figure 20 displays simulation results of the proposed modified vector control for the faulty IM in the difference values of reference speed. Figure 20(a) shows the reference and actual rotor speed, when the speed reference changes from 100 rpm to 700 rpm. In this figure a fault cut-off occurs at the starting. Figure 20(b) shows the speed error between reference speed and actual speed. It is evident from Figures 20(a) and 20(b) that the faulty IM can follow the reference speed without any overshoot and steady-state error. Figure 20(c) shows the electromagnetic torque of the motor in the faulty condition. It can be seen from the presented results that the dynamic performance of the proposed drive system is highly satisfactory.

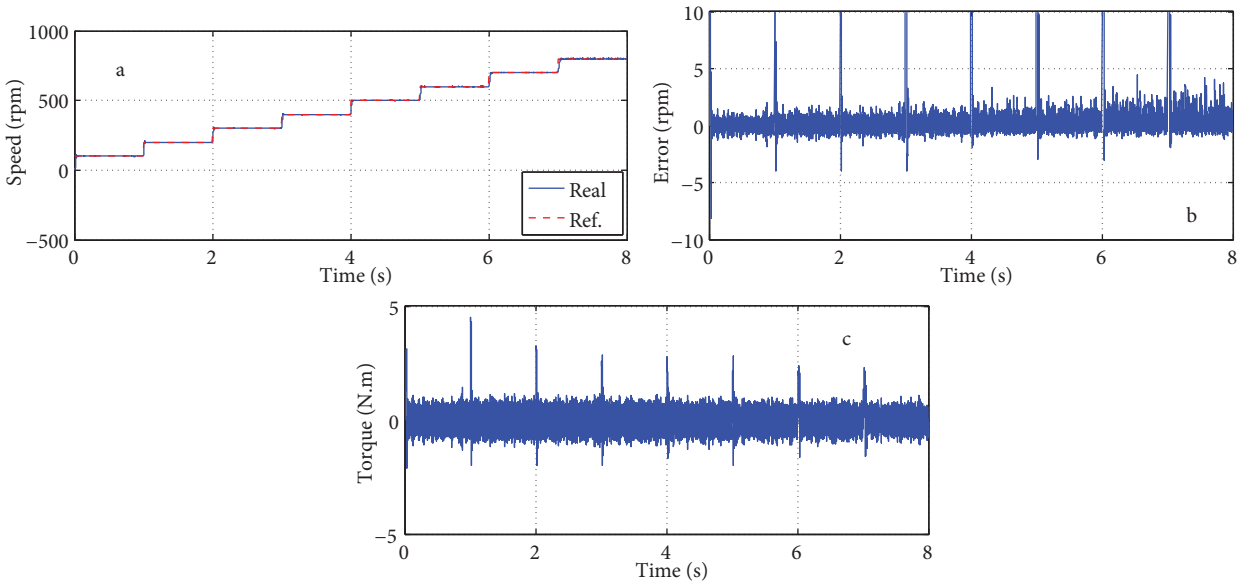

Figure 20. Simulation results of the modified controller in the difference values of reference speed; (a) Speed, (b) Speed error, (c) Electromagnetic torque.

7. Conclusion

In this paper, two methods for modeling (d-q and WFM) and a novel approach for the RFOC of a faulty three-phase IM fed by PWM, three-leg VSI, is recommended. In the presented technique, a GSA is implanted for tuning PI controllers. It can be shown that under fault condition, by using some changes in the block diagram of the conventional RFOC, we can control the unbalanced or faulty IM. It can be noted that the faulty IM structure is like a single-phase IM structure. It is envisaged that the presented technique for faulty IM control can be used for single-phase IMs as well.

References

[1] Bradley KJ, Tami A. Reluctance mesh modelling of induction motors with healthy and faulty rotors. In: Industry Applications Conference, 6–10 October 1996; San Diego, CA, USA: IEEE. pp. 625-632.

[2] Gerada C, Bradley K, Sumner M, Sewell P. Evaluation of a vector controlled induction motor drive using the dynamic magnetic circuit model. In: IEEE 2003 International Conference on Industry Applications; 12–16 October 2003; Salt Lake City, UT, USA: IEEE. pp. 1-8.

[3] Jannati M, Fallah E. Modeling and vector control of unbalanced induction motors (faulty three phase or single phase induction motors). In: IEEE 2010 The 1st Conference on Power Electronic & Drive Systems & Technologies; 17–18 February 2010; Tehran, Iran: IEEE. pp. 208-211.

[4] Jannati M, Idris NRN, Salam Z. A new method for modeling and vector control of unbalanced induction motors. In: IEEE 2012 Energy Conversion Congress and Exposition; 15–20 September 2012; Raleigh, NC, USA: IEEE. pp. 3625-3632.

[5] Jasim O, Gerada C, Sumner M, Arellano-Padilla J. Investigation of induction machine phase open circuit faults using a simpli?ed equivalent circuit model. In: IEEE 2008 International Conference on Electrical Machines; 6–9 September 2008; Vilamoura, Portugal: IEEE. pp. 1-6.

[6] Jasim O, Sumner M, Gerada C, Arellano-Padilla J. Development of a new fault-tolerant induction motor control strategy using an enhanced equivalent circuit model. IET Electr Power App 2011; 5: 618-625.

[7] Toliyat HA, Lipo TA, White JC. Analysis of a concentrated winding induction machine for Adjustable Speed Drive Applications-part I (Motor Analysis). IEEE T Energy Conver 1991; 6: 679-684.

[8] Toliyat HA, Lipo TA, White JC. Analysis of a concentrated winding induction machine for adjustable speed drive applications-part II (Motor design and performance analysis). IEEE T Energy Conver 1991; 6: 685-692.

[9] Slemon GR. Modeling of induction machines for electric drives. IEEE T Ind Appl 2002; 38: 101-109.

[10] Toliyat HA, Lipo TA. Transient analysis of cage induction machines under stator, rotor bar and end ring faults. IEEE T Energy Conver 1995; 10: 241-247.

[11] Nandi S, Toliyat HA. Novel frequency-domain-based technique to detect stator interturn faults in induction machines using stator-induced voltages after switch-off. IEEE T Ind Appl 2002; 38: 101-109.

[12] Milimonfared J, Kelk HM, Der Minassians A, Nandi S, Toliyat HA. A novel approach for broken rotor bar detection in cage induction motors. IEEE T Ind Appl 1999; 35: 1000-1006.

[13] Joksimovic MG, Penman J. The detection of inter-turn short circuits in the stator windings of operating motors. IEEE T Ind Electron 2000; 47: 1078-1084.

[14] Luo X, Liao Y, Toliyat H, El-Antably A, Lipo TA. Multiple coupled circuit modeling of induction machines. IEEE T Ind Appl 1995; 31: 311-318.

[15] Nandi S. Detection of stator faults in induction machines using residual saturation harmonics transient model for induction machines with stator winding turn faults. IEEE T Ind Appl 2006; 42: 1201-1208.

[16] Ghazal M, Poshtan J. Robust stator winding fault detection in induction motors. In: IEEE 2011 the 2nd Conference on Power Electronics, Drive Systems and Technologies; 16–17 February 2011; Tehran, Iran: IEEE. pp. 163-168.

[17] Eltabach M, Charara A, Zein I. A comparison of external and internal methods of signal spectral analysis for broken rotor bars detection in induction motors. IEEE T Ind Electron 2004; 5: 107-121.

[18] Aydin I, Karakose M, Akin E. A new method for early fault detection and diagnosis of broken rotor bars. Energ Convers Manage 2011; 52: 1790-1799.

[19] Wolbank TM, Wohrnschimmel R. On-line stator winding fault detection in inverter fed induction motors by stator current reconstruction. In: IET 1999 the 9th Conference on Electrical Machines and Drive; 1–3 September 1999; Canterbury, UK: IEEE. pp. 253-257.

[20] Tallam RM, Habetler TG, Harley RG. Transient model for induction machines with stator winding turn faults. IEEE T Ind Appl 2002; 38: 632-637.

[21] Tallam RM, Habetler TG, Harley RG, Gritter DJ, Burton BH. Neural network based on-line stator winding turn fault detection for induction motors. In: IEEE 2000 Conference in Industry Applications; 8–12 October 2000; Rome, Italy: IEEE. pp. 375-380.

[22] Tallam RM, Habetler TG, Harley RG. Transient model for induction machines with stator winding turn faults. In: IEEE 2000 Conference in Industry Applications; 8–12 October 2000; Rome, Italy: IEEE. pp. 304-309.

[23] Gaeta A, Scelba G, Consoli A. Modelling and control of three-phase PMSMs under open-phase fault. IEEE T Ind Appl 2013; 49: 74-83.

[24] Vas P. Vector Control of AC Machines. Oxford, UK: Oxford University Press, 1990.

[25] Zhao Y, Lipo TA. Modeling and control of a multiphase induction machine with structural unbalance, part I-machine modeling and multi-dimensional current regulation. IEEE T Energy Conver 1996; 3: 570-577.

[26] Zhao Y, Lipo TA. Modeling and control of a multiphase induction machine with structural unbalance, part II-field-oriented control and experimental verification. IEEE T Energy Conver 1996; 3: 578-584.

[27] Abbaszadeh K, Fallah E, Mili Monfared J. Modeling and simulation of dual three-phase induction machine under fault conditions and proposal of a new vector control approach for torque oscillation reduction. Sci Iran 2002; 9: 321-327.

[28] Formato RA. Central force optimization: a new nature inspired computational framework for multidimensional search and optimization. Stud Comp Intell 2008; 129: 221-238.

[29] Tang KS, Man KF, Kwong S, He Q. Genetic algorithms and their applications. IEEE Signal Proc Mag 1996; 13: 22-37.

[30] Farmer JD, Packard NH, Perelson AS. The immune system, adaptation and machine learning. Physica D 1986; 2: 187-204.

[31] Bergh FVD, Engelbrecht AP. A study of particle swarm optimization particle trajectories. Inform Sciences 2006; 176: 937-971.

[32] Hu W, Yen GG. Adaptive multiobjective particle swarm optimization based on parallel cell coordinate system. IEEE T Evolut Comput 2015; 19: 1-8.

[33] Kirkpatrick S, Gelatto CD, Vecchi MP. Optimization by simulated annealing. Science 1983; 220: 671-680.

[34] Dorigo M, Maniezzo V, Colorni A. The ant system: optimization by a colony of cooperating agents. IEEE T Syst Man Cyb 1996; 26: 29-41.

[35] Gazi V, Passino KM. Stability analysis of social foraging swarms. IEEE T Syst Man Cyb 2004; 34: 539-557.

[36] Kim DH, Abraham A, Cho JH. A hybrid genetic algorithm and bacterial foraging approach for global optimization. Inform Sciences 2007; 177: 3918-3937.

[37] Rashedi E, Nezamabadi-pour H, Saryazdi S. GSA: a gravitational search algorithm. Inform Sciences 2009; 179: 2232-2248.

[38] Badr A, Fahmy A. A proof of convergence for ant algorithms. Inform Sciences 2004; 160: 267-279.

[39] Ellabib I, Calamai P, Basir O. Exchange strategies for multiple ant colony system. Inform Sciences 2007; 177: 1248-1264.

[40] Hamzacebi C. Improving genetic algorithms' performance by local search for continuous function optimization. Appl Math Comput 2008; 196: 309-317.

[41] Lozano M, Herrera F, Cano JR. Replacement strategies to preserve useful diversity in steady-state genetic algorithms. Inform Sciences 2008; 178: 4421-4433.

[42] Tripathi PK, Bandyopadhyay S, Pal SK. Multi-objective particle swarm optimization with time variant inertia and acceleration coefficients. Inform Sciences 2007; 177: 5033-5049.

[43] Elbeltagi E, Hegazy T, Grierson D. Comparison among five evolutionary-based optimization algorithms. Adv Eng Inform 2005; 19: 43-53.

[44] Uysall O, Bulkan S. Comparison of genetic algorithm and particle swarm optimization for bicriteria permutation flowshop scheduling problem. Int J Comput Int Res 2008; 4: 159-175.

[45] Vesterstrom J, Thomsen R. A comparative study of differential evolution, particle swarm optimization, and evolutionary algorithms on numerical benchmark problems. In: IEEE 2004 Congress on Evolutionary Computation; 19–23 Jun 2004; Portland, OR, USA: IEEE. pp. 1980-1987.

[46] Liu H, Abraham A, Clerc M. Chaotic dynamic characteristics in swarm intelligence. Appl Soft Comput 2007; 7: 1019-1026.

[47] Biswas A, Dasgupta S, Das S, Abraham A. A synergy of differential evolution and bacterial foraging algorithm for global optimization. Neural Netw World 2007; 17: 607-626.

[48] Fitzgerald AE, Kingsley C, Umans SD. Electric Machinery. 6th ed. New York, NY, USA: McGraw-Hill, 2003.

[49] Saleh A, Pacas M, Shaltout A. Fault tolerant field oriented control of the induction motor for loss of one inverter phase. In: IEEE 2006 the 32nd Conference on Industrial Electronics; 6–10 November 2006; Paris, France; IEEE. pp. 817-822.

A. Appendix

Obtaining equation of faulty motor in the "abc" frame:

Voltage, flux and torque equations for faulty three-phase IM in the "abc" frame can be written as the following equations:

Stator and rotor voltage equations:

$$\begin{bmatrix} v_{abS}^{2\times1} \\ v_{abcR}^{3\times1} \end{bmatrix} = \begin{bmatrix} R_S^{2\times2} & 0^{2\times3} \\ 0^{3\times2} & R_R^{3\times3} \end{bmatrix} \begin{bmatrix} i_{abS}^{2\times1} \\ i_{abcR}^{3\times1} \end{bmatrix} + \frac{d}{dt} \begin{bmatrix} \lambda_{abS}^{2\times1} \\ \lambda_{abcR}^{3\times1} \end{bmatrix}$$

Stator and rotor flux equations:

$$\begin{bmatrix} \lambda_{abS}^{2\times1} \\ \lambda_{abcR}^{3\times1} \end{bmatrix} = \begin{bmatrix} L_{SS}^{2\times1} & L_{SR}^{2\times3} \\ L_{SR}^{2\times3T} & L_{RR}^{3\times3} \end{bmatrix} \begin{bmatrix} i_{abS}^{2\times1} \\ i_{abcR}^{3\times1} \end{bmatrix}$$

Torque equation:

$$\tau_e = \frac{Pole}{2}[i_{abS}]^T[\frac{\partial L_{SR}}{\partial \theta_r}][i_{abcR}],$$

where $[v_{abcR}]$, $[i_{abcR}]$, $[\lambda_{abcR}]$, $[R_R]$, and $[L_{RR}]$, are identical to the balanced three-phase IM. It is because the structure of the rotor has not changed. The $[v_{abS}]$, $[i_{abS}]$, $[\lambda_{abS}]$, $[R_S]$, $[L_{SS}]$, $[L_{SR}]$, and $[L_{RS}]$ have similar formation to the balanced IM. The only difference in these matrixes is the row and column for the phase "c $_s$" are removed.

Obtaining equation of faulty motor in the d-q frame

Applying the transformation vectors ($[T_S]$ and $[T_r]$), stator and rotor voltages and fluxes can be written as the following equations:

$$\begin{aligned}
[v_{dqs}^s] &= [T_S][R_S][T_S]^{-1}[i_{dqs}^s] + [T_S]\tfrac{d}{dt}\left([T_S]^{-1}[\lambda_{dqs}^s]\right) \\
[\lambda_{dqs}^s] &= [T_S][L_{SS}][T_S]^{-1}[i_{dqs}^s] + [T_S][L_{SR}][T_r]^{-1}[i_{dqr}^s] \\
[v_{dqr}^s] &= [T_r][R_R][T_r]^{-1}[i_{dqr}^s] + [T_r]\tfrac{d}{dt}\left([T_r]^{-1}[\lambda_{dqr}^s]\right) \\
[\lambda_{dqr}^s] &= [T_r][L_{RR}][T_r]^{-1}[i_{dqr}^s] + [T_r][L_{RS}][T_S]^{-1}[i_{dqs}^s] \\
\tau_e &= \tfrac{Pole}{2}\left([T_S]^{-1}[i_{dqs}^s]\right)^T[\tfrac{\partial L_{SR}}{\partial \theta_r}]\left([T_r]^{-1}[i_{dqr}^s]\right)
\end{aligned}$$

By simplifying above equation, the equations of faulty motor with different stator windings in a stationary reference frame (superscript "s") can be expressed as Eqs. (4)–(9):

The matrixes R_s, R_r, L_{ss}, L_{sr}, and L_{rr} in the WFM are defined as follows:

$$[R_r] = \begin{bmatrix} 2(R_b+R_e) & -R_b & 0 & \dots & 0 & -R_b \\ -R_b & 2(R_b+R_e) & -R_b & \cdots & 0 & 0 \\ \cdots & \cdots & \cdots & \cdots & \cdots & \cdots \\ 0 & 0 & 0 & \dots & 2(R_b+R_e) & -R_b \\ -R_b & 0 & 0 & \dots & -R_b & 2(R_b+R_e) \end{bmatrix}$$

$$[R_s] = r_s \,.\, I_{3\times 3} = \begin{bmatrix} r_s & 0 & 0 \\ 0 & r_s & 0 \\ 0 & 0 & r_s \end{bmatrix} \quad [L_{ss}] = \begin{bmatrix} L^s_{11} & L^s_{12} & L^s_{13} \\ L^s_{21} & L^s_{22} & L^s_{23} \\ L^s_{31} & L^s_{32} & L^s_{33} \end{bmatrix} \quad [L_{sr}] = \begin{bmatrix} L^{sr}_{11} & L^{sr}_{12} & \dots & L^{sr}_{1m} \\ L^{sr}_{21} & L^{sr}_{22} & \dots & L^{sr}_{2m} \\ L^{sr}_{31} & L^{sr}_{32} & \dots & L^{sr}_{3m} \end{bmatrix}$$

$$[L_{rr}] = \begin{bmatrix} L_{mr} + 2\left(L_b + L_e\right) & L_{r_1r_2} - L_b & L_{r_1r_3} & \dots & L_{r_1r_m} - L_b \\ L_{r_2r_1} - L_b & L_{mr} + 2\left(L_b + L_e\right) & L_{r_2r_3} - L_b & \dots & L_{r_2r_m} \\ L_{r_3r_1} & L_{r_3r_2} - L_b & L_{mr} + 2\left(L_b + L_e\right) & \dots & L_{r_3r_m} \\ \dots & \dots & \dots & \dots & \dots \\ L_{r_mr_1} - L_b & L_{r_mr_2} & L_{r_mr_3} & \dots & L_{mr} + 2\left(L_b + L_e\right) \end{bmatrix}$$

In these matrixes, $[R_s]$ is a diagonal m by m consisting of resistances of each coil, and $[R_r]$ is n+1 by n+1 symmetric where R_b is the rotor bar resistance and R_e is the end ring segment resistance. The matrix $[L_{ss}]$ is a symmetric m by m matrix. The mutual inductance matrix $[L_{sr}]$ is an m by n matrix composed of the mutual inductances between the stator coils and the rotor loops. L_{mr} is the magnetizing inductance of each rotor loop. L_b is the rotor bar leakage inductance. Le is the rotor end ring leakage inductance and $L_{r_ir_k}$ is the mutual inductance between two rotor loops.

B. Appendix

Equations of faulty IM by using proposed rotational transformations:

Torque equation:	Rotor voltage equations:
$\tau_e = \frac{Pole}{2}\left(M_q i^s_{qs} i^s_{dr} - M_d i^s_{ds} i^s_{qr}\right)$ $= \frac{Pole}{2}\begin{bmatrix} i^s_{dr} & i^s_{qr} \end{bmatrix}\begin{bmatrix} 0 & M_q \\ -M_d & 0 \end{bmatrix}\begin{bmatrix} i^s_{ds} \\ i^s_{qs} \end{bmatrix}$ $= \left(\frac{Pole}{2}\begin{bmatrix} i^s_{dr} & i^s_{qr} \end{bmatrix}[T^e_s]^T\left([T^e_s]^{-1}\right)^T \begin{bmatrix} 0 & M_q \\ -M_d & 0 \end{bmatrix}[T^e_{is}]^{-1}[T^e_{is}]\begin{bmatrix} i^s_{ds} \\ i^s_{qs} \end{bmatrix}\right)$ $= \frac{Pole}{2} M_q\left(i^e_{qs} i^e_{dr} - i^e_{ds} i^e_{qr}\right)$	$[T^e_s]\begin{bmatrix} 0 \\ 0 \end{bmatrix} = [T^e_s]\begin{bmatrix} M_d\frac{d}{dt} & \omega_r M_q \\ -\omega_r M_d & M_q\frac{d}{dt} \end{bmatrix}[T^e_{is}]^{-1}[T^e_{is}]\begin{bmatrix} i^s_{ds} \\ i^s_{qs} \end{bmatrix}$ $+ [T^e_s]\begin{bmatrix} r_r + L_r\frac{d}{dt} & \omega_r L_r \\ -\omega_r L_r & r_r + L_r\frac{d}{dt} \end{bmatrix}[T^e_s]^{-1}[T^e_s]\begin{bmatrix} i^s_{dr} \\ i^s_{qr} \end{bmatrix}$ $= \begin{bmatrix} M_q\frac{d}{dt} & -\left(\omega_e - \omega_r\right)M_q \\ \left(\omega_e - \omega_r\right)M_q & M_q\frac{d}{dt} \end{bmatrix}\begin{bmatrix} i^e_{ds} \\ i^e_{qs} \end{bmatrix}$ $+ \begin{bmatrix} r_r + L_r\frac{d}{dt} & -\left(\omega_e - \omega_r\right)L_r \\ \left(\omega_e - \omega_r\right)L_r & r_r + L_r\frac{d}{dt} \end{bmatrix}\begin{bmatrix} i^e_{dr} \\ i^e_{qr} \end{bmatrix}$

Stator voltage equations:

$$[T^e_{vs}]\begin{bmatrix} v^s_{ds} \\ v^s_{qs} \end{bmatrix} = [T^e_{vs}]\begin{bmatrix} r_s + L_{ds}\frac{d}{dt} & 0 \\ 0 & r_s + L_{qs}\frac{d}{dt} \end{bmatrix}[T^e_{is}]^{-1}[T^e_{is}]\begin{bmatrix} i^s_{ds} \\ i^s_{qs} \end{bmatrix}$$
$$+ [T^e_{vs}]\begin{bmatrix} M_d\frac{d}{dt} & 0 \\ 0 & M_q\frac{d}{dt} \end{bmatrix}[T^e_s]^{-1}[T^e_s]\begin{bmatrix} i^s_{dr} \\ i^s_{qr} \end{bmatrix} \Rightarrow$$

$$\begin{bmatrix} v_{ds}^e \\ v_{qs}^e \end{bmatrix} = \begin{bmatrix} r_{qs} + L_{qs}\frac{d}{dt} & -\omega_e L_{qs} \\ \omega_e L_{qs} & r_{qs} + L_{qs}\frac{d}{dt} \end{bmatrix} \begin{bmatrix} i_{ds}^e \\ i_{qs}^e \end{bmatrix} + \begin{bmatrix} M_q\frac{d}{dt} & -\omega_e M_q \\ \omega_e M_q & M_q\frac{d}{dt} \end{bmatrix} \begin{bmatrix} i_{dr}^e \\ i_{qr}^e \end{bmatrix}$$

$$+ \begin{bmatrix} \begin{pmatrix} (\frac{M_q^2}{M_d^2}r_{ds} - r_{qs}) + \\ (\frac{M_q^2}{M_d^2}L_{ds} - L_{qs})\frac{d}{dt} \end{pmatrix} & -\omega_e(\frac{M_q^2}{M_d^2}L_{ds} - L_{qs}) \\ \omega_e(\frac{M_q^2}{M_d^2}L_{ds} - L_{qs}) & \begin{pmatrix} (\frac{M_q^2}{M_d^2}r_{ds} - r_{qs}) + \\ (\frac{M_q^2}{M_d^2}L_{ds} - L_{qs})\frac{d}{dt} \end{pmatrix} \end{bmatrix} \begin{bmatrix} i_{ds}^{-e} \\ i_{qs}^{-e} \end{bmatrix}$$

where

$$\begin{bmatrix} i_{ds}^{-e} \\ i_{qs}^{-e} \end{bmatrix} = \begin{bmatrix} \cos^2\theta_e & -\sin\theta_e\cos\theta_e \\ -\sin\theta_e\cos\theta_e & \sin^2\theta_e \end{bmatrix} \begin{bmatrix} i_{ds}^e \\ i_{qs}^e \end{bmatrix}$$

C. Appendix

The ratings and parameters of three-phase IM are:

Voltage: 125 V, f = 50 Hz, No. of poles = 4, Power = 475 W, $J = 0.0038$ kg.m^2, $r_s = 20.6\ \Omega$, $L_{lr} = L_{ls} = 0.0814$ H, $r_r = 19.15\ \Omega$, $L_{ms} = 0.851$ H